

Effects of Shear Wave Velocity Profile of Soil on Seismic Response of High Rise Buildings

Navid Yeganeh^{a*}; Behzad Fatahi^a; and Sergei Terzaghi^b

^a *School of Civil and Environmental Engineering, University of Technology Sydney (UTS), Sydney, Australia*

^b *ARUP Australia, Sydney Office, Australia*

*Navid.Yeganeh@uts.edu.au

Abstract

There is, nowadays, a conspicuous demand for the high rise buildings in the high-density dwellings of the urban areas; in consequence, harnessing the whiz-bang numerical simulations plus conducting the rigorous experimental studies so as to design and construct such prodigious structures would be essential. Thus, the appropriate parameters for modeling the structure and the soil medium in the Soil-Structure Interaction (SSI) system should be selected. The soil-structure interaction is referred to the process in which the soil response is told on by the structure motion whilst the latter is affected by the soil motion. The current research zeroed in on the soil shear wave velocity and its influence on the superstructure performance. Invoking the weighted average shear wave velocity with the aim of calculating the soil shear modulus, which is closely related to the strength and deformation characteristics of the soil, has been a hotly debated issue since the aforesaid parameter was posited by a plethora of codes and regulations to obtain the soil site classification required for the earthquake design. To that end, the numerical model, having two assorted profiles associated with the shear wave velocity, namely, the in situ non-uniform profile (Case A) and the equivalent uniform profile (Case B), was built by means of FLAC3D, capable of analyzing the complex interaction issues via the direct method whereby the entire system of the structure-foundation-soil is modeled and analyzed in one single step. To put it in a nutshell, employing the weighted average shear wave velocity for the entire soil mass in parsing of the 3D seismic soil-structure interaction problems would be accused for ending up with somewhat unreliable results, e.g., underestimated drift ratio and building deformation, which might be the culprit of the damage to the building and possibly the death of the residents residing in the earthquake-prone zones.

Keywords: Soil-structure interaction, Weighted average shear wave velocity, High rise building, Seismic analysis, FLAC3D.

1. Introduction

Soil-structure interaction is an interdisciplinary field of science which encompasses soil and structural mechanics and dynamics, earthquake engineering, geophysics, geomechanics, mathematical-numerical methods, technical fields, and so forth. Generally speaking, the structure is considered fixed-base in calculating the force implemented by earthquake on the structure, disregarding the flexibility of the soil under the structure. Nevertheless, the past experiences and observations [1-3] have indicated the fact that the soil deformation changes the characteristics of the free field motion at the ground level, in addition to altering the structure reaction against earthquake. As a general rule, the soil-structure interaction yields the certain results such as a diminishment in the base shear but an escalation in the structure period (or reduction of the frequency), the system damping, and contribution of the rocking mode to the total response. Yet, it is daunting to clearly discuss as regards the P- Δ effect and lateral displacements of the structures in default of conducting the interaction analysis for each project [4].

Be it geotechnical or structural design situations, the Dynamic Soil-Structure Interaction (DSSI) plays a fundamental role to the extent that the unexpected damage might befall, e.g., stemming from

resonance; in contrast, DSSI might act as a precursor to the soil-foundation relative displacement markedly abating the energy that reaches the superstructure, reducing the expected damage. Furthermore, the analysis methods, involved in the soil-structure interaction, can be divided to two principal categories, viz, the direct and multi-step/substructure methods. In the former, which is mightily advantaged with the possibility of assuming the nonlinear behavior for the soil and structure materials along with the possibility of modeling the complex geometries, the entire system of the structure-foundation-soil is modeled and analyzed in one single step. It is to be noted that the aforementioned nonlinear effects must be computed with the response history analyses performed in the time domain [5-7].

It is not unfair to accentuate that one of the prime problems in the earthquake engineering is the definition of the seismic environment supposed to be harnessed in the analysis and design of the structures. The potential amplification of the ground motion is due to the characteristics of the near-surface rock or soil, particularly the stiffness characterized by the seismic shear wave velocity. It is now widely accepted that, throughout agitation, i.e. earthquake, the local site conditions may strikingly affect the rock-like motions and that soil-structure interaction phenomena would, in turn, alter the free field ground motions. The most spectacular cases of the soil amplification and soil-structure interaction effects have been observed in 1906 San Francisco, 1985 Mexico City, 1989 Loma Prieta, 1994 Northridge, 2010 Maule, and 2011 Tohoku earthquakes [8,9].

The fundamental problem, motivated the study in this paper, is that leveraging the constant average value of the shear wave velocity for the whole soil medium with the intention of estimating the soil stiffness, which has been déjà vu, courtesy of the pretense of simplicity, would beget ending up with a non-conservative design in the seismic analyses of the soil-structure interaction systems.

In the current paper, the nonlinearities of the superstructure, the soil mass, and the geometry, i.e. uplifting, gapping and P- Δ effect, were taken into consideration in the time-history analysis of the numerical model via FLAC3D. Besides, the Mohr-Coulomb soil constitutive model accompanied by the hysteretic damping, covering the backbone curve and Masing's rules, were assigned to the soil.

2. Numerical Simulation Using FLAC3D

The current research project made use of the direct method by employing FLAC3D, as finite difference software being used in the engineering mechanics computation, providing the wide-ranging optional facilities for modeling the soil-structure interaction problems as compared to the other geotechnical software.

2.1 Modeling the structural frame and the building foundation

A 20-story (60 m height), 3-span (12 m length) reinforced concrete moment-resisting building frame was considered as illustrated in Fig. 1. SAP2000-V14 was utilized for the structural design purpose in full compliance with AS/NZS1170.1-2002 [10], and AS3600-2009 [11], plus AS1170.4-2007 [12]. It should be stated that in the final selection of the beam and column sections, constructability and norms were heeded. Moreover, the modulus of elasticity of concrete and the Poisson's ratio were 3.01×10^{10} N/m² and 0.2, consecutively. The thickness of the concrete slabs was 0.25 m. The mass density of reinforced concrete was equal to 2400 kg/m³. It is worth underscoring that all the structural sections of the superstructure were analyzed in FLAC3D on the basis of the inelastic method, assuming the elastic-perfectly plastic behavior by specifying the limiting plastic moments for the structural elements giving rise to a discontinuity in the rotational motion, called a plastic hinge. Further, the effects of the cracking associated with the structural components, considering the type of the structural system (unanchored bending frame), were regarded to be 0.25, 0.35 and 0.7 [13] times the bending stiffness of their uncracked sections corresponding with the reduction of the stiffness of the slabs, beams, and columns.

The building foundation had a thickness of 1 m and a width of 14 m modeled by means of the finite difference zones having the bulk modulus, the shear modulus, and the mass density of 1.67×10^{10} N/m², 1.25×10^{10} N/m², and 2400 kg/m³, respectively.

It is manifest that the necessity of utilizing the damping in the dynamic problems is undeniable; as a consequence, the local damping coefficient of 0.157, engendering 5% damping, was considered for

the building and foundation thereto thanks to the fact that the local damping is a rational approximate way for including the hysteretic behavior in the seismic analyses [14].

It is desirable to represent a plane between a foundation and the underneath soil on which sliding and/or separation, i.e. uplift, could take place amidst the seismic excitation. In this realm, the crude rule of thumb for assessing the maximum interface stiffness values, shown in Eq. (1) [14], is that k_n , named the normal spring stiffness, and k_s , called the shear spring stiffness, should be set to ten times the equivalent stiffness of the stiffest neighboring zone.

$$k_n = k_s = 10 \times \max \left[\frac{K + \left(\frac{4}{3}\right)G}{\Delta z_{\min}} \right] \quad (1)$$

Where, K and G are the bulk and shear moduli of a neighboring zone, respectively, and Δz_{\min} is the smallest width of an adjoining zone in the normal direction to the interface.

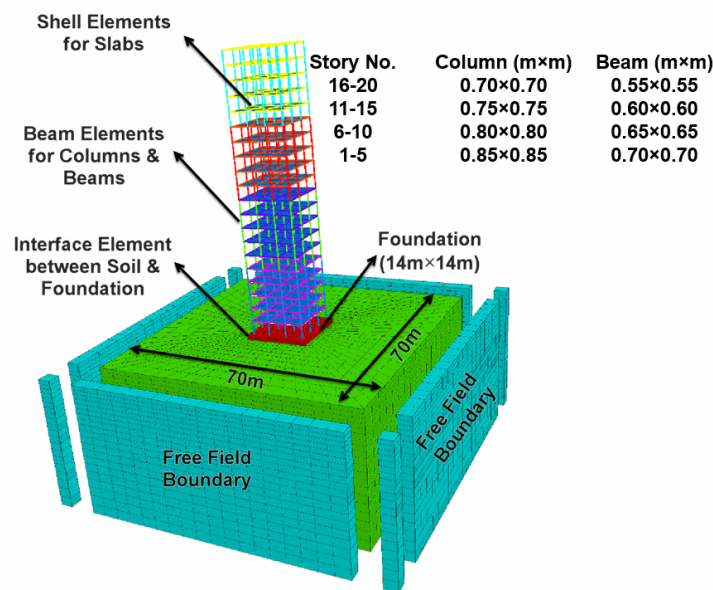


Fig. 1. Illustration of the soil-structure interaction system in the direct method

2.2 Soil constitutive model

The generalized relationship between stress and strain, linking the equations of equilibrium and compatibility, is termed “soil constitutive model”. The nonlinear Mohr-Coulomb model is an elastic-perfectly plastic yardstick plus the hysteretic damping as a supplement, simulating the inelastic cyclic behavior inasmuch as in soil and rock the natural damping is mainly hysteretic, implying that it is independent of frequency, which has been capitalized on by dozens of researchers (e.g. [15-17]) so as to mimic the soil behavior under the seismic loading in the soil-structure interaction system. In order to determine the hysteretic damping in the dynamic analysis of the current research, the two-variable function, named “Default model”, ($L_1 = -3.156$ & $L_2 = 1.904$) [14] was employed which is able to replicate the soil stiffness degradation with shear strain. Additionally, the soil parameters, involved in the said constitutive model, were as follows; friction angle = 29° , cohesion = 20 kPa, dilation angle = 5° , and density = 1900 kg/m³.

2.3 Boundary conditions and the input earthquake record

The free field boundaries, exemplified in Fig. 1, were applied at the side boundaries of the soil mass generating the one-dimensional free field wave propagation in parallel with the main-grid analysis;

henceforth, the plane waves, propagating upward, undergo no distortion at the boundaries as the free field grids supply the conditions identical to those in an infinite model. It is of note that the free field model encompasses four plane free field grids on the side boundaries of the model to match the main-grid zones, and four column free field grids at the corners acting as the free field boundaries for the plane free field grids. It is noteworthy to point out that the main rationale behind why a rigid boundary was adopted at the assumed bedrock level is to simulate the large dynamic impedance demystifying the low velocity sediments sitting on the high velocity bedrock.

The seismic acceleration record attributed to the 1994 Northridge earthquake appertaining to the Rinaldi station, cherry-picked from the Strong-Motion Virtual Data Center (VDC), depicted in Fig. 2, was applied to the base of the numerical model subsequent to the baseline correction, while conducting a nonlinear time-history analysis.

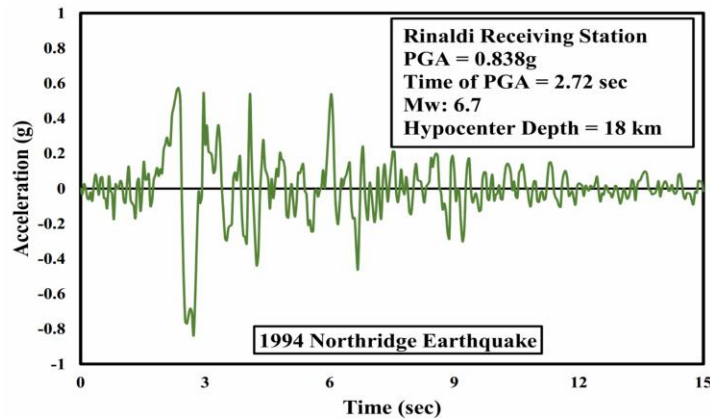


Fig. 2. Utilized earthquake base motion

2.4 Adopted shear wave velocity profiles

The characterization of the maximum small-strain shear modulus (G_{\max}) accompanying the shear wave velocity (V_s) of the soils and rocks would be an integral component of various seismic analyses, including hazard analysis, site classification, and site response analysis, plus soil-structure interaction. The seismic site classification is, by and large, carried out with the use of the weighted average of the shear wave velocity via Eq. (2) [18], which is calculated as the time for a shear wave to travel from a depth of 30 m to the ground surface, not the arithmetic average of V_s to a depth of 30 m. Albeit the estimation of the earthquake response spectra in accordance with the local soil site effects and the adopted field-based shear wave velocity profile would be the momentous part and parcel of the design of the new structures, plus the performance assessment and rehabilitation of the existing buildings.

$$\bar{V}_s = \frac{\sum_{i=1}^n d_i}{\sum_{i=1}^n \left(\frac{d_i}{V_{si}} \right)} \quad (2)$$

Where, d_i is the thickness of any layers from 0 to 30 m depth, and V_{si} is the shear wave velocity of each layer between 0 and 30 m depth.

At this juncture, perusing the nature and extend of the weighted average shear wave velocity in the calculation of the soil stiffness, which is all-important in the direct method, and the springs stiffness under a foundation used in the multi-step method, is indispensable. Consequently, the dynamic response of a high rise building in the soil-structure interaction model, having two assorted profiles associated with the shear wave velocity, viz, the in situ non-uniform profile (Case A) and the equivalent uniform profile (Case B) obtained from Eq. (2), was scrutinized so as to shed light on the possibility and importance thereunto of applying the weighted average of the shear wave velocity not only in the seismic site classification but also in defining the shear modulus of the soil medium. In that light, Fig. 3 portrays the abovementioned cases.

It is deemed necessary to lay emphasis on the needfulness of considering the interaction effects, particularly for the moment-resisting frames [19], once the shear wave velocity of the supporting soil is less than 600 m/s.

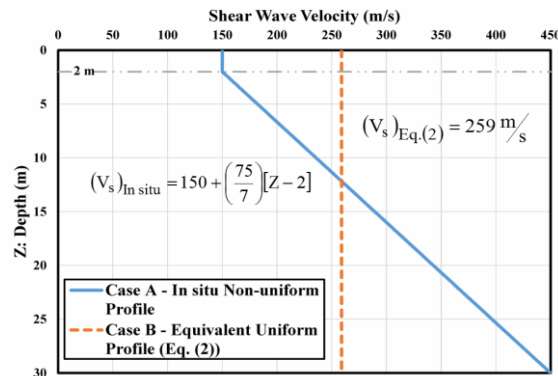


Fig. 3. Shear wave velocity profiles of interest

3. Results and Discussions

The structural results, embodying the base shear, the distributed shear force along the structure, the maximum lateral displacement, and the inter-story drift, plus the response spectrum, attributed to Cases A and B (see Fig. 3), were thoroughly parsed and presented in this section. As to the majority of the seismic codes and standards, e.g. ASCE/SEI 7-10 [18] and AS1170.4-2007 [12], considering a 30 m depth for the seismic bedrock is a ramification of transpiring the chief part of the amplification and/or attenuation in the aforesaid depth.

3.1 Shear force distribution along the building height

Inasmuch as the base shear as well as the shear force distribution along the superstructure height are per se at the forefront of designing any buildings, the absolute maximum shear force, experienced at each level during the earthquake excitation, ought to be reckoned by summing up the generated shear forces, resulting from the relative movement between the columns and slabs, in all columns at the level in question in every time increment in the midst of a time-history analysis. As it is discerned in Fig. 4, the distribution of the absolute maximum shear force for Case B showed a little resemblance to that of Case A even though the difference in the base shear values of Cases A and B is minor. The reason behind such an insignificant difference, which is around 0.55 MN, could be parsed via the response spectra, exhibited in Fig. 5, by checking out the values of the response acceleration (S_a) based on the vibration period of the soil-structure system including the building and the underneath soil, having different shear wave velocity profiles, which were roughly more than 2 seconds.

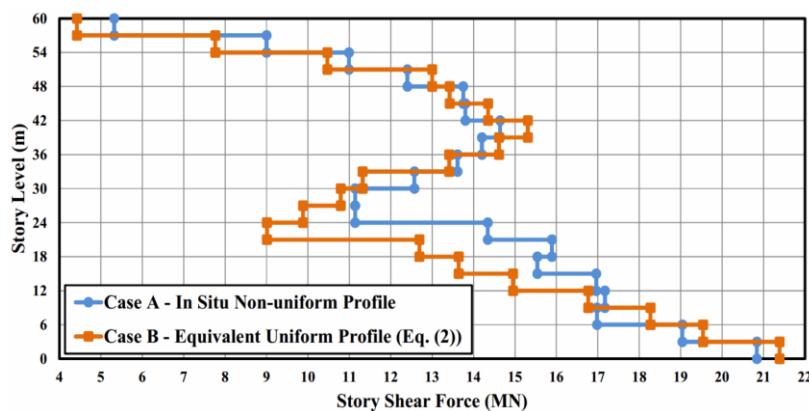


Fig. 4. Maximum shear force distribution under the influence of the Northridge (Rinaldi) earthquake

Forthrightly speaking, the fluctuation, displayed in Fig. 4, which happened in the shear force distribution along the structure, could be undoubtedly called a volte-face because the traditional engineering practice has only focused on the first translational mode of the vibration when setting the strength requirements and lateral force distributions; however, it is common for the response of a tall building to a strong ground shaking to be heavily influenced by the complex dynamic behavior, including the impacts of the higher modes of vibration.

3.2 Response spectra

Stated brief, the response spectra are plots expressing the maximum response for a Single-Degree-Of-Freedom (SDOF) system subjected to a specified excitation. The construction of such plots requires the solution of the single-degree-of-freedom systems for a sequence of values of the natural frequency and of the damping ratio in the range of interest. Every solution dispenses only one point (i.e. maximum value) of the response spectrum. Once the curves are constructed for the applied excitation, the seismic analysis for the design of the structure is declined to a simple calculation of the natural frequency (or period) of the system as well as the use of the response spectrum [20].

Nowadays, the amplification of the rock motion at the base of a structure amid the transmission through the overlying soil is common knowledge. It is hereby asserted that more energy would reach the foundation of the superstructure in Case A whose stiffness, all told, did not outweigh that of Case B owing to the lack of damping coming into picture. Using the handy rule of thumb that the fundamental period of an N-story building is approximately $N/10$ sec [21], it is crystal clear that the surface acceleration, whilst making a comparison between Case A and Case B, would be more or less detrimental, provided that a low rise building is placed on the site; whereas a 20-story building was considered in the current project.

Chandler et al. [22] postulated that the effective site period can be shifted to a considerably higher value, under the seismic condition, because of the degradation in the soil shear stiffness emerging from the seismically-induced straining in the soil. With due attention to Fig. 5, the point herein is that by escalating the number of stories in addition to accounting for the period-lengthening effect of the soil-structure interaction system throughout a strong earthquake in view of the descent in the stiffness arising from the structural damage, a negligible difference could be seen between the cases in question.

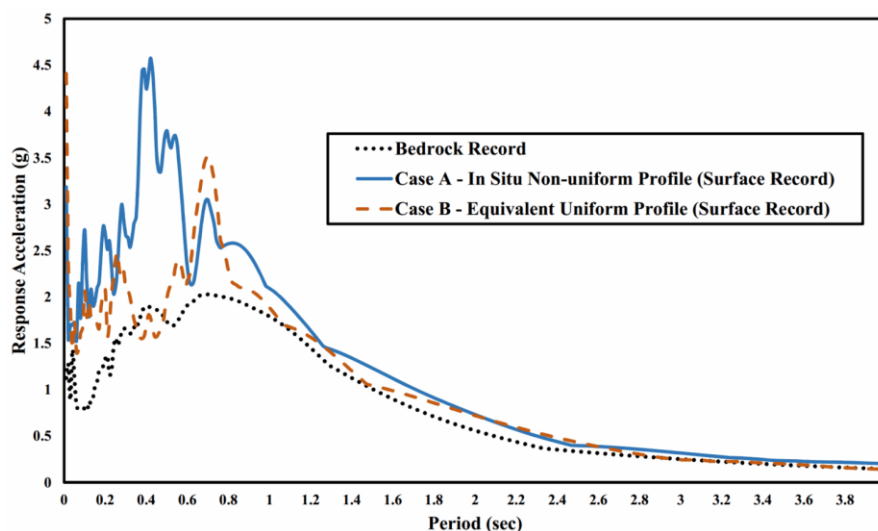


Fig. 5. Acceleration response spectra, with 5% damping ratio for the structure, associated with a selected point right beneath the foundation

3.3 Flooring Lateral displacements and the inter-story drifts

In spite of the fact that there have been pros and cons apropos of the second-to-none estimation methodology attributed to the lateral displacement and drift ratio thereof through a time-history analysis, the lateral displacement of each story, when the maximum occurs at the top level, i.e. roof, would

demonstrate a more tangible pattern of the structure deformation by comparison with the pattern casting light on the absolute maximum displacement of all stories regardless of the time of the occurrence. Strictly speaking, the lateral displacement of roof has an irresistible role in the calculation of the minimum separation gap between the neighboring structures. The results connected with the maximum inter-story drifts and lateral displacements, graphically indicated in Figs. 6 and 7, could be encapsulated as below.

The criterion, being exploited here, is the structural performance, named “Life Safety” (LS) [23], which is a combination of the performance of the both structural and non-structural components, revolving around the post-earthquake damage state in which some structural elements are severely damaged. Having said that, the large falling debris hazards either within or outside the building would not come off. It should be borne in mind that the injuries might be ineluctable during the earthquake; even so, it is expected that the overall risk of the life-threatening injury as a result of the structural damage is low. In full compliance with the said touchstone, the total transient story drift ratio must remain less than 2% to satisfy the Life Safety performance level. The drift ratio of Case B satisfied the yardstick in all building levels; quite the contrary, that of Case A in the upper levels surpassed such that the inter-story drift ratio of 2.5% was reached. This is paramount in light of the fact that the ascent in the lateral displacement and thus boosting the story drift ratio would be the culprit of the upsurge concomitant with the P- Δ effect arousing a condition of the instability under the gravity loads. Referring to Figs. 6 and 7, the inter-story drifts generally follow the same pattern as the lateral deflections.

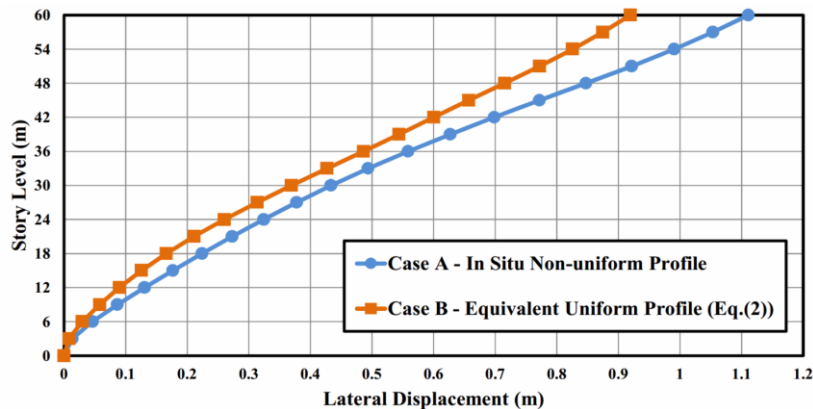


Fig. 6. Maximum lateral displacement of the 20-story structure under the influence of the Northridge (Rinaldi) earthquake

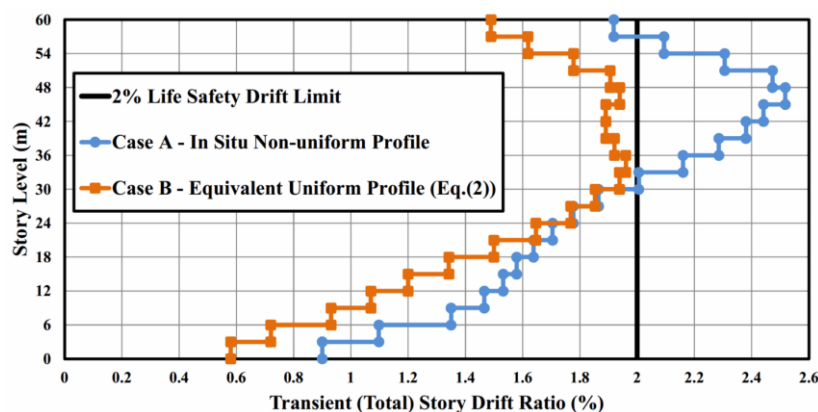


Fig. 7. Inter-story drift of the 20-story structure under the influence of the Northridge (Rinaldi) earthquake

4. Conclusions

In the contemporary era, a growing demand of the high rise buildings, characterizing the skyline of a typical modern megacity, in the urban areas is abundantly evident. There is a scarcity of research allocated to the analysis of the interaction connected with the shear wave velocity profile type on the

seismic response of reinforced concrete moment-resisting building frames. Therefore, a 3D soil-structure model was numerically developed, adopting the direct method of analysis. Indeed, the shear wave velocity is a valuable indicator of the dynamic properties of soils on account of its direct relation with the small-strain shear modulus. It can be generally mentioned that a soil constitutive model for the dynamic soil-structure interaction analysis is supposed to be able to capture the hysteresis curves and the energy-absorbing characteristic. Those were fulfilled by leveraging the Mohr-Coulomb model plus the hysteretic damping feature embedded in FLAC3D software.

The shear demand and the story drift of a superstructure would be the essence of sifting the seismic response of a building frame. The results disclosed that the influence of the shear wave velocity profile type on the base shear plus the distributed shear along the building height could be almost disregarded for the adopted 20-story building. Contrariwise, the story drift ratio, defined as the lateral story displacement divided by the story height, demystified that applying the weighted average shear wave velocity in lieu of making use of the adopted field-based profile sparked off the aggressive (unsafe) design of a building due to exceeding the 2% yardstick hinging around the Life Safety performance level which was posited for the rehabilitation of the existing structures.

Needless to say, the response spectrum of the ground motion, recorded at the base of the structure, spells out the impact of the soil-structure interaction on the soil movement. The response spectra connected with Case A (i.e. the in situ non-uniform profile) and Case B (i.e. the equivalent uniform profile) in the short-period range were distinguishable in order that the aftereffects of considering the profile, delineated in Case A, might be harrowing, with the provision that a low rise building exists on the site studied in this paper.

Even though putting the weighted average shear wave velocity into practice with the purpose of evaluating the seismic site classification accompanying computing the small-strain shear modulus, which is typically associated with the strains on the order of $10^{-3}\%$ or less, in advance of running a dynamic analysis, tends to simplify the mathematical analysis of the problem, it was concluded, in line with the outcomes derived from the current research, that the aforesaid procedure is an oversimplification of reality, implying that the actual shear wave velocity profile resulting from the field measurements ought to be directly utilized in the seismic analysis of structures.

References

- [1] Tabatabaiefar HR, Fatahi B. Idealisation of soil-structure system to determine inelastic seismic response of mid-rise building frames. *Soil Dynamics and Earthquake Engineering*2014;66:339-351.
- [2] Hokmabadi AS, Fatahi B. Influence of foundation type on seismic performance of building considering soil-structure interaction. *International Journal of Structural Stability and Dynamics*2016;16:1550043(1-29).
- [3] Nguyen QV, Fatahi B, Hokmabadi AS. Influence of size and load-bearing mechanism of piles on seismic performance of buildings considering soil-pile-structure interaction. *International Journal of Geomechanics*2017;17(7):04017007(1-22).
- [4] Yeganeh N, Bazaz JB, Akhtarpour A. Seismic analysis of the soil-structure interaction for a high rise building adjacent to deep excavation. *Soil Dynamics and Earthquake Engineering*2015;79:149-170.
- [5] Chu D. Three-dimensional nonlinear dynamic analysis of soil-pile-structure interaction. PhD, Washington: Washington University; 2006.
- [6] Abate G, Massimino MR, Maugeri M, Wood DM. Numerical modelling of a shaking table test for soil-foundation-superstructure interaction by means of a soil constitutive model implemented in a FEM code. *Geotechnical and Geological Engineering*2010;28(1):37-59.
- [7] NEHRP Consultants Joint Venture. NIST GCR 12-917-21: Soil-structure interaction for building structures. Gaithersburg: US Department of Commerce; 2012.
- [8] Romo MP. Clay behavior, ground response and soil-structure interaction studies in Mexico City. In: International conferences on recent advances in geotechnical earthquake engineering and soil dynamics. St. Louis; 2-7 April 1995.
- [9] Xia J, Miller RD, Park CB. Estimation of near-surface shear-wave velocity by inversion of Rayleigh waves. *Geophysics*1999;64(3):691-700.

- [10] Australian/New Zealand Standard. AS/NZS1170.1: Structural design actions-part 1: permanent, imposed and other actions. Sydney: Standards Australia/Standards New Zealand; 2002.
- [11] Australian Standard. AS3600: Concrete structures. Sydney: Standards Australia; 2009.
- [12] Australian Standard. AS1170.4: Structural design actions-part 4: earthquake actions in Australia. Sydney: Standards Australia; 2007.
- [13] ACI Committee. ACI 318-14: Building code requirements for structural concrete and commentary. Farmington Hills: American Concrete Institute; 2014.
- [14] Itasca. User's manual FLAC3D: fast lagrangian analysis of continua in 3 Dimensions, version 5.0. Minneapolis: Itasca Consulting Group; 2014.
- [15] Conniff DE, Kioussis PD. Elastoplastic medium for foundation settlements and monotonic soil-structure interaction under combined loadings. *International Journal for Numerical and Analytical Methods in Geomechanics*2007;31(6):789-807.
- [16] Rayhani M, El Naggar M. Physical and numerical modeling of seismic soil-structure interaction in layered soils. *Geotechnical and Geological Engineering*2012;30(2):331-342.
- [17] Walton HJ, Davids WG, Landon ME, Clapp JD. Simulation of buried arch bridge response to backfilling and live loading. *Journal of Bridge Engineering*2016;21(9):04016052-1-11.
- [18] ASCE Standard. ASCE/SEI 7-10: Minimum design loads for buildings and other structures. Reston: American Society of Civil Engineers; 2010.
- [19] Tabatabaiefar SHR, Fatahi B, Samali B. Seismic behavior of building frames considering dynamic soil-structure interaction. *International Journal of Geomechanics*2013;13(4):409-420.
- [20] Paz M. *Structural dynamics: theory and computation*. Norwell: Kluwer Academic Publishers; 2004.
- [21] Bungale ST. *Tall building design steel, concrete, and composite systems*. Boca Raton: CRC Press-Taylor & Francis Group; 2016.
- [22] Chandler A, Lam N, Sheikh MN. Response spectrum predictions for potential near-field and far-field earthquakes affecting Hong Kong soil sites. *Soil Dynamics and Earthquake Engineering*2002;22(6):419-440.
- [23] Applied Technology Council (ATC). *National Earthquake Hazards Reduction Program (NEHRP) guidelines for the seismic rehabilitation of buildings, (FEMA 273)*. Washington DC: Federal Emergency Management Agency; 1997.